




# Past and Future of a Type Ia Supernovae Progenitor Candidate HD 265435

Wei-Zhong Qi<sup>1,2</sup>, Dong-Dong Liu<sup>1,2</sup>, and Bo Wang<sup>1,2</sup> 

<sup>1</sup> Yunnan Observatories, Chinese Academy of Sciences, Kunming 650216, China; [liudongdong@ynao.ac.cn](mailto:liudongdong@ynao.ac.cn), [wangbo@ynao.ac.cn](mailto:wangbo@ynao.ac.cn)

<sup>2</sup> University of Chinese Academy of Sciences, Beijing 100049, China

Received 2022 June 23; revised 2022 November 2; accepted 2022 November 7; published 2022 December 9

## Abstract

As one of the most useful cosmological distance indicators, type Ia supernovae (SNe Ia) play an important role in the study of cosmology. However, the progenitors of SNe Ia are still uncertain. It has been suggested that carbon-oxygen white dwarf (CO WD)+He subgiant systems could produce SNe Ia through the double-degenerate (DD) model, in which the He subgiant transfers He-rich matter to the primary CO WD and finally evolves to another CO WD. Recently, a CO WD+He star system (i.e., HD 265435) has been discovered to be a new SNe Ia progenitor candidate based on the DD model. The orbital period of the system is about 0.0688 days, and the masses of the CO WD and the He star are  $1.01 \pm 0.15 M_{\odot}$  and  $0.63^{+0.13}_{-0.12} M_{\odot}$ , respectively. In this work, we evolve a large number of primordial binaries to the formation of CO WD+He star systems and investigate the evolutionary history of HD 265435. We find that HD 265435 may originate from a primordial binary that has a  $5.18 M_{\odot}$  primary and a  $3.66 M_{\odot}$  secondary with an initial orbital period of 5200 days. The CO WD+He star system would be formed after the primordial binary experiences two common-envelope ejection processes. We also find that HD 265435 would evolve to a double WD system with a total mass of  $1.58 M_{\odot}$  after a stable mass-transfer process, and the double WD system would merge driven by gravitational wave radiation. We estimate that it would take about 76 Myr for HD 265435 to form an SN Ia. In addition, HD 265435 would be a potential target of space-based gravitational wave observatories (e.g., LISA, Taiji and TianQin).

*Key words:* (stars:) binaries (including multiple): close – stars: individual (HD 265435) – stars: evolution – (stars:) supernovae: general – (stars:) white dwarfs

## 1. Introduction

Supernovae (SNe) are among the most violent phenomena in the Universe, in which type Ia supernovae (SNe Ia) are characterized by the absence of hydrogen and helium lines in spectra near the maximum luminosity (see Filippenko 1997). Due to the high luminosity and the significant uniformity of SNe Ia, they are regarded as standard cosmological distance indicators, which leads to the important discovery that the Universe is expanding at an accelerating rate (e.g., Riess et al. 1998; Perlmutter et al. 1999). Besides, SNe Ia play an important role in the chemical evolution of galaxies, since more than half of the iron group in their host galaxies originate from SN Ia explosions (e.g., Greggio & Renzini 1983; Matteucci & Greggio 1986). Additionally, SNe Ia are accelerators of cosmic rays (e.g., Fang & Zhang 2012). However, the progenitors of SNe Ia are still uncertain, which may have great influence on the accuracy of the detected cosmological distances (e.g., Podsiadlowski et al. 2008; Liu et al. 2012; Wang & Han 2012; Wang et al. 2013; Maoz et al. 2014). So far, many progenitor models of SNe Ia have been proposed, among which the most popular models are the single-degenerate (SD) model and the double-degenerate (DD) model.

In the SD model, a carbon-oxygen white dwarf (CO WD) increases its mass by accreting hydrogen-rich or helium-rich material from a non-degenerate companion. When the mass of the WD approaches to the Chandrasekhar (Ch) mass limit, an SN Ia explosion is assumed to occur (Whelan & Iben 1973; Nomoto 1982; Li & van den Heuvel 1997). The companion could be a main-sequence (MS) star, a red giant star or a helium (He) star (e.g., Hachisu et al. 1996; Li & van den Heuvel 1997; Langer et al. 2000; Han & Podsiadlowski 2004; Chen & Li 2007; Wang et al. 2009b; Chen & Li 2009; Wang & Han 2010b; Liu et al. 2010; Ablimit et al. 2014; Liu et al. 2019; Ablimit & Maeda 2019; Ablimit 2022; Xu et al. 2022). In this case, the homogeneity of most SNe Ia can be naturally explained. Furthermore, the synthetic spectra from the SD Ch mass model could fit well with the early spectra for most SNe Ia (e.g., Nomoto et al. 1984; Hoefflich et al. 1996; Nugent et al. 1997). In addition, the SD model is also supported by some other observational clues, like the early optical and ultraviolet (UV) emission from ejecta-companion interaction in some SNe Ia (e.g., Kasen 2010; Ganeshalingam et al. 2011; Wang et al. 2012; Liu et al. 2015; Cao et al. 2015; Marion et al. 2016), the signatures of circumstellar matter before SN explosion (e.g., Patat et al. 2007; Wang et al. 2009c; Sternberg et al. 2011;

Dilday et al. 2012; Silverman et al. 2013), the wind-blown cavity in some SN remnants (e.g., Badenes et al. 2007; Williams et al. 2011) and the possible pre-explosion images (e.g., Voss & Nelemans 2008; McCully et al. 2014), etc.

In the DD model, the merger of two WDs may lead to an SN Ia if the total mass of double WDs is larger than the Ch mass (Tutukov & Yungelson 1981; Webbink 1984; Iben & Tutukov 1984). It has been found that the DD model could well reproduce the birthrates and delay time distribution of SNe Ia (e.g., Nelemans et al. 2001; Mennekens et al. 2010; Liu et al. 2018b). The observed delay time distribution following the power-law distribution with an index of  $-1$  may reflect correlations between the SN Ia rates and galaxy properties (e.g., Maoz & Mannucci 2012; Graur et al. 2017). Besides, many other observational evidences favor the DD model, like the absence of H or He lines in the nebular spectra of most SNe Ia (e.g., Leonard 2007; Ganeshalingam et al. 2011), the existence of super-luminous SNe Ia whose total mass of progenitor  $\geq 2 M_{\odot}$  (e.g., Howell et al. 2006; Hicken et al. 2007; Scalzo et al. 2010; Silverman et al. 2011), no signature of ejecta-companion interaction in some SNe Ia (e.g., Olling et al. 2015), no definite evidence for surviving companion stars of SNe Ia (e.g., Badenes et al. 2007; Kerzendorf et al. 2009; Schaefer & Pagnotta 2012) and no early radio emissions detected (e.g., Hancock et al. 2011; Horesh et al. 2012), etc. However, instead of a thermonuclear explosion, the merger of two WDs may result in the formation of a neutron star through accretion-induced collapse events (e.g., Nomoto & Iben 1985; Liu & Wang 2020). Fortunately, the accretion-induced collapse could be avoided in some parameter ranges (e.g., Yoon et al. 2007; Pakmor et al. 2011; Liu et al. 2016).

It has been suggested that the CO WD+He subgiant systems could produce SNe Ia via both the SD model and the DD model. In the SD model, the CO WD would accrete material from the He subgiant. The material is He-rich and would burn into C and O to increase the mass of CO WD (e.g., Yoon & Langer 2003; Wang et al. 2009a, 2017). This channel is proposed to explain SNe Ia with short delay times (Wang et al. 2009b). In the DD model, the CO WD accumulates He-rich matter from the He subgiant and finally a double massive WD system would be formed (e.g., Ruiters et al. 2013; Liu et al. 2016). Recently, Liu et al. (2018b) found that the observed delay time distribution of SNe Ia can be well reproduced after considering the WD+He subgiant channel based on the DD model, especially at early epochs ( $< 1$  Gyr) and old epochs ( $> 8$  Gyr) where there is a deficiency.

There are many observational clues which can be used to constrain progenitor models of SNe Ia, among which searching for progenitor candidates is very useful. For the CO WD+He subgiant channel, HD 49 798 with its companion and V445 Pup are both progenitor candidates based on the SD model. The former consists of a  $1.50 \pm 0.05 M_{\odot}$  subdwarf O6 star and a  $1.28 \pm 0.05 M_{\odot}$  compact companion (e.g., Israel et al. 1997;

Wang & Han 2010a; Mereghetti et al. 2016; Liu et al. 2018a; Chen 2022). The later is the only known He nova containing a  $> 1.35 M_{\odot}$  CO WD without trace of neon observed in the nebular-phase spectrum (e.g., Ashok & Banerjee 2003; Kato & Hachisu 2003; Woudt & Steeghs 2005). For the WD+He subgiant channel of the DD model, the only known progenitor candidate is KPD 1930+2752 (e.g., Maxted et al. 2000; Geier et al. 2007). Liu et al. (2018b) suggested that KPD 1930+2752 would evolve to a double WD system without going through any mass-transfer process, and would produce an SN Ia when the double WDs merge. Recently, Pelisoli et al. (2021) reported a new SN Ia progenitor candidate HD 265435 at the distance of 445 pc. HD 265435 contains a  $1.01 \pm 0.15 M_{\odot}$  CO WD and a  $0.63_{-0.12}^{+0.13} M_{\odot}$  sdB star with an orbital period of 0.068 818 488 8 days, which is located within the parameter space of WD+He subgiant systems for producing SNe Ia shown in Liu et al. (2018b). However, the evolutionary history of HD 265435 remains unknown.

In the present work, we evolve a large number of primordial binaries to the formation of CO WD+He star systems, and provide the most representative evolution trace for HD 265435. In Section 2, we introduce the basic assumptions and numerical methods used in the present work. The corresponding results are presented in Section 3. A discussion and a summary are finally given in Section 4.

## 2. Numerical Methods

By combining the rapid evolutionary code (Hurley et al. 2002) and Monte Carlo method, we simulate the evolution of primordial binaries to the formation of CO WD+He star systems. In every simulation, we evolve  $10^7$  primordial binaries. Some basic hypotheses and initial parameters are listed as follows:

1. We assume that all stars are members of binaries and their orbits are circular.
2. The prescription from Miller & Scalo (1979) is adopted to describe the initial mass function of primordial primaries.
3. The initial mass ratio ( $q = M_2/M_1$ ) is regarded as a constant distribution, i.e.,  $n(q) = 1$ .
4. We adopt the solar metallicity  $Z = 0.02$  in our simulation, which is also the best fitting metallicity for HD 265435 in Pelisoli et al. (2021).
5. For the orbital separations, we assume that the distribution is constant in  $\log a$  for wide binaries, and falls off smoothly for close binaries (for details see Han et al. 1995).

Common envelope (CE) evolution plays a key role in the formation of WD+He star systems, but the CE ejection process remains a mystery (e.g., Ivanova et al. 2013). The relationship between the orbital energy and the binding energy is commonly used to parameterize the CE interaction. In the present work,

we use the standard energy prescription to investigate the outcome of the CE stage (Webbink 1984). This prescription contains two uncertain parameters: the CE ejection efficiency ( $\alpha_{\text{CE}}$ ) and the stellar structure parameter ( $\lambda$ ). In our standard model,  $\lambda$  is set to be 0.5 and  $\alpha_{\text{CE}}$  is adopted to be 1.0. The influence of different  $\alpha_{\text{CE}}$  is also discussed in Section 4.

Recently, gravitational wave (GW) has become another important messenger since the first GW event of double black hole merger was detected by the ground-based GW observatories LIGO/Virgo (Abbott et al. 2016). In addition, many space-based GW observatories are under scheduled, like LISA, TianQin and Taiji (Danzmann & LISA Study Team 1997; Luo et al. 2016; Hu & Wu 2017). Compared with ground-based observatories, they have the ability to detect the GW at lower frequency. In the present work, we would explore whether the semidetached CO WD+He star systems can be detected by these space-based GW observatories. The GW frequency of binaries is defined as  $f_{\text{GW}} = 2/P_{\text{orb}}$ ,  $P_{\text{orb}}$  is the orbital period of the binary. The chirp mass of CO WD+He star system is calculated by the prescription written as:

$$M_{\text{chirp}} = \frac{(M_{\text{WD}}M_{\text{He}})^{3/5}}{(M_{\text{WD}} + M_{\text{He}})^{1/5}}, \quad (1)$$

where  $M_{\text{WD}}$  and  $M_{\text{He}}$  are the masses of the white dwarf and the He star.

In principle, Equation (1) can be only used in detached binaries, where the orbital decay is fully caused by the GW radiation. However, the mass-transfer within the binary also affects the orbital evolution. Tauris (2018) defined a dynamical chirp mass to deal with the issue and in some cases there may be a negative chirp mass. Note that Equation (1) could still represent the order of magnitude of chirp mass when the mass transfer is driven by GW radiation and occurs on a timescale close to that of GWs.

Considering the mission lifetime of  $T = 4$  yr for LISA, we adopt the characteristic strain of GW described in Chen (2020), which is suitable for binaries with circular orbits, written as:

$$h_c \approx 2.5 \times 10^{-20} \left( \frac{f_{\text{GW}}}{1 \text{mHz}} \right)^{7/6} \left( \frac{M_{\text{chirp}}}{1 M_{\odot}} \right)^{5/3} \left( \frac{15 \text{kpc}}{d} \right) \quad (2)$$

where  $d$  is the distance between the binary and a detector. In this work, the distance  $d$  is adopted to be 0.4549 kpc, which is the distance of HD 265435. We will also qualitatively discuss the influence of a various distance on the results in Section 4.

After the formation of double WD system, they would get closer and eventually merge. During the process, we adopted an assumption that the orbital contraction of the double WDs is completely driven by GW radiation, i.e., the tidal interaction between the two components is ignored. The timescale for this process is calculated as follows:

$$\tau = 47.9 \frac{(M_{\text{WD1}} + M_{\text{WD2}})^{1/3}}{M_{\text{WD1}}M_{\text{WD2}}} (P_{\text{orb}}/\text{day})^{8/3} \text{Gyr}, \quad (3)$$

where  $M_{\text{WD1}}$  and  $M_{\text{WD2}}$  are the masses of two WDs in  $M_{\odot}$  in the binary (Kraft et al. 1962).

### 3. Results

#### 3.1. Evolutionary Channels

There are mainly four evolutionary channels to form CO WD+He star systems distinguished by the phases of two stars when systems evolve to the first CE phase, as follows:

Channel A: In this channel, the initial masses of primaries ( $M_1^i$ ) range from 2.5 to 9.5  $M_{\odot}$ , the initial mass ratios ( $q^i = M_2^i/M_1^i$ ) are in the range of  $0.2 \leq q^i \leq 0.9$  and the initial orbital periods ( $P_{\text{orb}}^i$ ) range from 2.5 to 35 days. The primary expands rapidly when it evolves to the red giant branch (RGB) stage, leading to a stable Roche-lobe overflow (RLOF) process. After the mass-transfer process, the primary exhausts its H shell and becomes a He star. The primary continues to evolve and will fill its Roche-lobe again at the He subgiant stage. In this case, the mass-transfer is also dynamically stable. After the second mass-transfer process, the He-rich layer of the primary is exhausted and the binary turns to a CO WD+MS system. Subsequently, the secondary evolves to the RGB and fills its Roche-lobe. Because of the dynamically unstable mass-transfer, a CE is formed. After the CE ejection, a CO WD+He star system is left behind. The parameters of the formed CO WD+He star systems are in the range of  $0.4 M_{\odot} \leq M_{\text{WD}} \leq 1.5 M_{\odot}$ ,  $0.3 M_{\odot} \leq M_{\text{He}} \leq 3.5 M_{\odot}$  and  $0.01 \text{ days} \leq P_{\text{orb}} \leq 0.3 \text{ days}$ .

Channel B: The parameters of the primordial binaries are in the range of  $M_1^i \sim 1.0\text{--}6.5 M_{\odot}$ ,  $q^i \sim 0.9\text{--}1.0$  and  $P_{\text{orb}}^i \sim 630\text{--}4500$  days. The primary fills its Roche-lobe when it evolves to the early asymptotic giant branch (EAGB) or the thermally-pulsing asymptotic giant branch (TPAGB) stage and the secondary evolves to the RGB stage. In this case, a double-core CE would be formed because of the dynamically unstable mass-transfer. If the CE could be ejected, the binary becomes a CO WD+He star system. The parameters of the formed CO WD+He star systems are in the range of  $0.5 M_{\odot} \leq M_{\text{WD}} \leq 1.2 M_{\odot}$ ,  $0.3 M_{\odot} \leq M_{\text{He}} \leq 1.5 M_{\odot}$  and  $0.02 \text{ days} \leq P_{\text{orb}} \leq 0.4 \text{ days}$ .

Channel C: The parameters of the primordial binaries are in the range of  $M_1^i \sim 2.0\text{--}6.5 M_{\odot}$ ,  $q^i \sim 0.3\text{--}0.9$  and  $P_{\text{orb}}^i \sim 1800\text{--}6300$  days. Similar to Channel B, the primary also has to evolve to the TPAGB stage to fill its Roche-lobe, while the secondary is still a main sequence. At this stage, the mass transfer is dynamically unstable and a CE would be formed. After the CE ejection, the primary becomes a CO WD. When the secondary evolves to the RGB or TPAGB stage, it fills its Roche-lobe and enters a second CE phase. If the CE can be ejected, the binary turns to a CO WD+He star system. The parameters of the formed CO WD+He star systems are in the

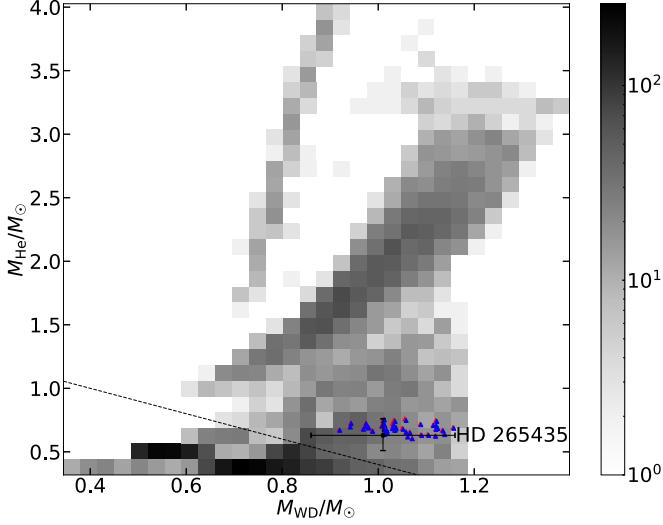


**Figure 1.** Distribution of CO WD+He binaries in WD mass–He star mass ( $M_{\text{WD}} - M_{\text{He}}$ ) panel. The black dot with error bars represents the position of HD 265435. Triangles represent samples that have  $M_{\text{WD}}$  and  $M_{\text{He}}$  within the error bars of HD 265435. The dashed line shows the position where the total mass equals to the Chandrasekhar mass. The intensity of the black-white bar represents the number of CO WD + He star systems in each bin.

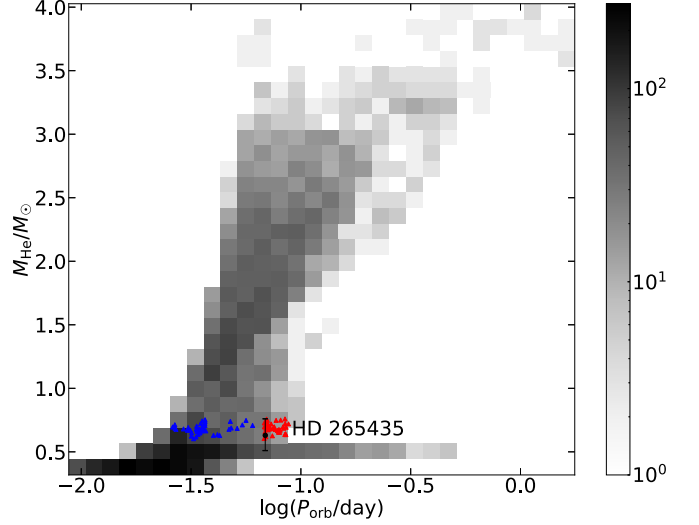


**Figure 2.** Similar to Figure 1, but in  $\log P_{\text{orb}} - M_{\text{He}}$  panel. Red triangles represent the CO WD+He star systems that are just formed, whereas blue triangles are the corresponding RLOF CO WD+He star/He subgiant systems (for details see Section 3.3).

range of  $0.5 M_{\odot} \leq M_{\text{WD}} \leq 1.2 M_{\odot}$ ,  $0.3 M_{\odot} \leq M_{\text{He}} \leq 1.0 M_{\odot}$  and  $0.01 \text{ days} \leq P_{\text{orb}} \leq 0.1 \text{ days}$ .

Channel D: The parameters of the primordial binaries are in the range of  $M_1^i \sim 4.5\text{--}8.0 M_{\odot}$ ,  $q^i \sim 0.7\text{--}1.0$  and  $P_{\text{orb}}^i \sim 10\text{--}25$  days. This channel is similar to Channel A until the primary evolves to a He star. After that, the secondary fills its Roche-lobe when the binary evolves to a He star+HG/RGB star system. At this stage, a double-core CE would be formed due to dynamically unstable mass transfer. If the CE can be ejected, a CO WD+He star system is produced. The parameters of the formed CO WD+He star systems are in the range of  $0.5 M_{\odot} \leq M_{\text{WD}} \leq 1.0 M_{\odot}$ ,  $1.0 M_{\odot} \leq M_{\text{He}} \leq 3.8 M_{\odot}$  and  $0.04 \text{ days} \leq P_{\text{orb}} \leq 0.8 \text{ days}$ .

### 3.2. Distributions of CO WD+He Star Systems

Figure 1 provides a distribution of CO WD+He star systems when they just evolve into the CO WD+He star phase in the  $M_{\text{WD}} - M_{\text{He}}$  panel. The masses of WDs range from  $0.4 M_{\odot}$  to about  $1.3 M_{\odot}$  and the masses of He stars are in the range of  $0.5 M_{\odot}\text{--}4.0 M_{\odot}$ . From this figure, we can see that the density is higher where  $M_{\text{tot}} < M_{\text{Ch}}$  and the number of CO WD+He star systems in that area is even more than half of total number. This is caused by the initial mass function, i.e., the number of stars increases when the initial masses decrease. Figure 2 represents the distribution of CO WD+He star systems in the  $\log P_{\text{orb}} - M_{\text{He}}$  panel. From this figure, we can see that CO WD+He star systems have orbital periods ranging from 0.01 to 1 day. Note that CO WD+He star systems with longer orbital

periods tend to have more massive He stars. This result can be explained by the CE ejection prescription: a more massive He star corresponds to a less orbital energy release.

### 3.3. Evolutionary History and Future Evolution of HD 265435

We assume that CO WD+He star binaries could produce HD 265435 if they satisfy the following conditions:

1. The masses of two components are within the observational error of HD 265435, which means  $M_{\text{WD}}$  is in the range of  $0.86\text{--}1.16 M_{\odot}$  and  $M_{\text{He}}$  ranges from  $0.51 M_{\odot}$  to  $0.76 M_{\odot}$ .
2. When binaries just evolve to CO WD+He star phase (red triangles in Figures 1 and 2),  $P_{\text{orb}}$  should be larger than or similar to the observed orbital period of HD 265435 (0.0688184888 days).
3. When CO WD+He star systems evolve to be semidetached (blue triangles in Figures 1 and 2),  $P_{\text{orb}}$  should be smaller than or similar to the observed orbital period of HD 265435.

We totally obtain 42 CO WD+He star systems that satisfy the conditions above. Almost all of them correspond to the evolutionary Channel C shown in Section 3.1. We use the least squares method to select the most representative sample and thus obtain the possible evolutionary history of HD 265435 shown in Figure 3. In the beginning, the primordial binary consists of two zero-age main sequences, a  $5.18 M_{\odot}$  primary and a  $3.66 M_{\odot}$  secondary, with an initial orbital period  $P_{\text{orb}} \approx 5200$  days (stage 1). After about 111 Myr, the primary

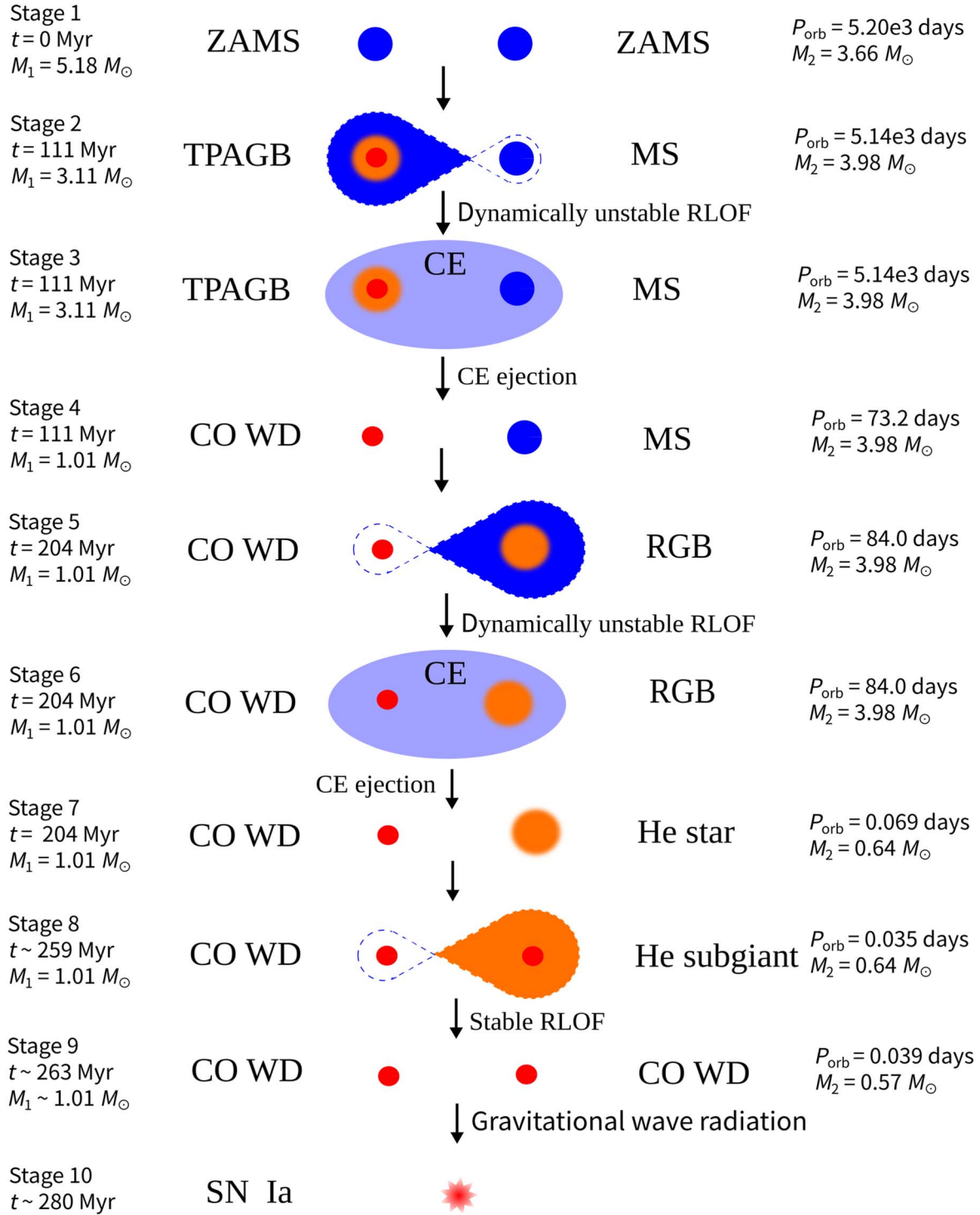
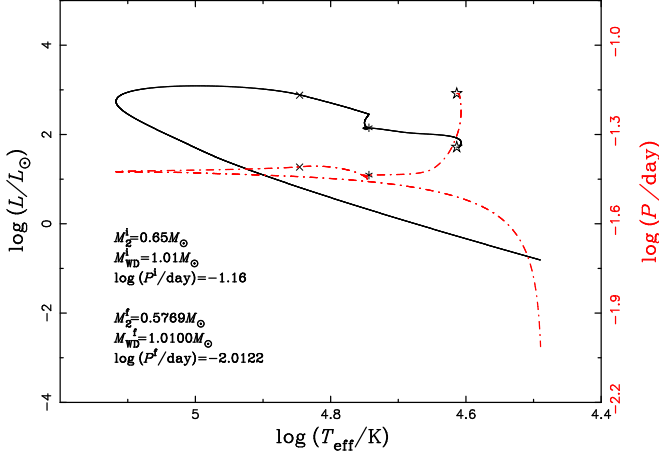


Figure 3. The evolutionary history and future evolution of HD 265435.



**Figure 4.** Evolutionary track of the binary from stage 7 to 9 in Figure 3. The solid curve and the red dashed–dotted curve represent the evolution of the luminosity of the secondary and the orbital period as a function of effective temperature, respectively. The pentagrams represent the position where our simulation starts. The asterisks and the crosses represent the beginning and the end of mass transfer, respectively.

evolves to a  $3.11 M_{\odot}$  TPAGB star which contains a  $1.01 M_{\odot}$  CO core and fills its Roche-lobe (Stage 2). As the mass-transfer process is dynamically unstable, the first CE is formed (stage 3). After the CE ejection, the primary becomes a  $1.01 M_{\odot}$  CO WD and the secondary is still a main sequence with the orbital period shrinking to 73.2 days (stage 4). At  $t = 204$  Myr, the secondary expands quickly and fills its Roche-lobe at the RGB stage (stage 5). In this case, the mass-transfer phase is also dynamically unstable, leading to the formation of the second CE (stage 6). After the CE ejection, the binary consists of a  $1.01 M_{\odot}$  CO WD and a  $0.64 M_{\odot}$  He star with an orbital period of 0.069 days (stage 7).

Figure 4 shows the evolutionary track from stage 7 to 9 in Figure 3, which is simulated by employing Eggleton’s stellar evolution code (Eggleton 1973; Han et al. 1994; Pols et al. 1995, 1998; Eggleton & Kiseleva-Eggleton 2002). Note that the luminosity and effective temperature are both higher than the observed data at the beginning of Figure 4. The main reason for this discrepancy is that a thin hydrogen envelope maybe exist on the surface of the hot subdwarf star in HD 265435, which would lead to lower effective temperature and luminosity. The existence of such a thin hydrogen envelope would not have strong influence on the binary evolution (see Pelisoli et al. 2021). During the CO WD+He star phase, the orbital period would decrease due to GW radiation. At  $t = 259$  Myr, the secondary becomes a He subgiant that contains a CO-core and expands to fill its Roche-lobe. Then the He subgiant starts to transfer He-rich material as well as angular momentum to the WD. In this case, the orbital period tends to become longer, contending with GW radiation (stage 8). As a result, it leads to a stabilization of orbital period for

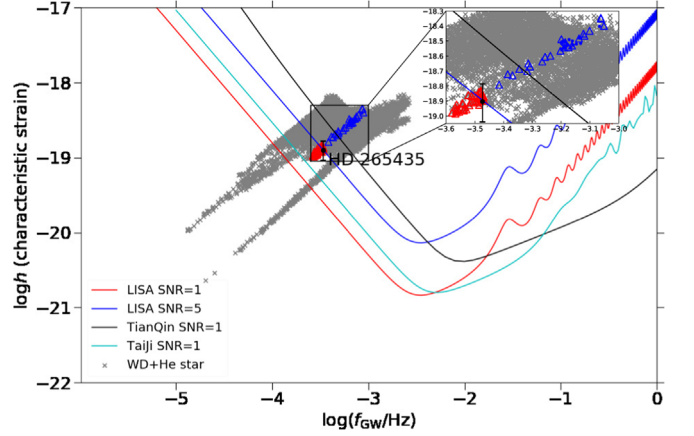


**Figure 5.** The characteristic strains of different CO WD+He binaries. We rudely assume that the distance is 0.455 kpc, which is consistent with the distance of HD 265435. Grey crosses represent all CO WD+He star systems in stage 7 in Figure 3. Red and blue data have the similar meaning as those in Section 3.3.

about 4 Myr, i.e., the almost horizontal part of the red dashed–dotted curve in Figure 4. When the He-rich layer of the secondary is exhausted, the system contains two CO WDs, and the mass of the new formed WD is  $0.57 M_{\odot}$  (stage 9). In this stage, there is no mass exchange and GW radiation dominates again, leading to the lose of orbital angular momentum. Finally, we estimate that the double WD system would merge and produce an SN Ia explosion at  $t = 280$  Myr (stage 10).

#### 4. Discussion and Summary

Recently, the GW signal has become an important way to study the properties of binaries. Figure 5 displays the GW characteristic strains of CO WD+He star binaries in the  $\log h - \log f_{\text{GW}}$  plane. From this figure, we can see that the GW frequencies of CO WD+He star binaries range from  $\sim 10^{-5}$  Hz to  $\sim 10^{-2.5}$  Hz, and their GW characteristic strains are in the range of  $10^{-21} \sim 10^{-18}$ . The red and blue data in this figure represent the systems that could produce HD 265435, similar to the red and blue triangles in Section 3.3. Note that the blue dots represent systems whose secondaries are He main sequences when they fill Roche-lobe and their secondaries are He subgiants for the blue triangles. We also present the sensitive curves of some future space-based GW observatories, like LISA, TianQin and Taiji in Figure 5. We can see that HD 265435 is located on the sensitive curve of LISA SNR = 5, which means that the system is detectable as a low-frequency GW source at present and in its future evolution. In the present work, the distance is simply set to be 455 pc. If we enlarge the distance, like 8.5 kpc, the systems in Figure 5 would move downward overall and there are still several semidetached binaries that are over the SNR = 5 sensitive curves of LISA.

We define HD 265435-like systems as CO WD+He star systems that could evolve to double WD phase and merge to

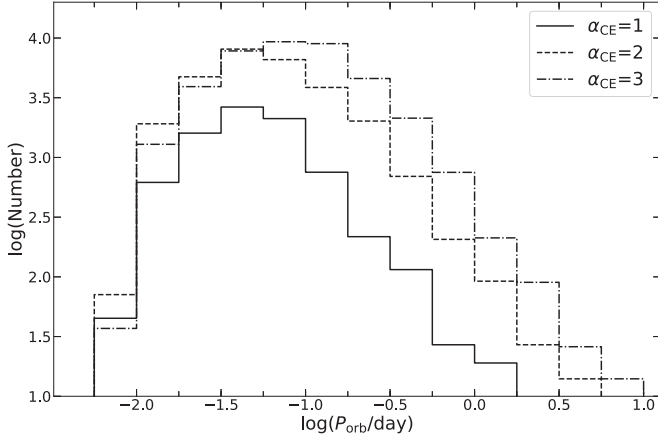


**Figure 6.** Orbital period distributions of CO WD+He star systems for different values of  $\alpha_{CE}$ .

produce SNe Ia. To estimate the number of this kind of systems, we adopted the Galactic birth rate of SN Ia from the WD+He subgiant channel provided by Liu et al. (2018b), which is about  $0.8\text{--}3.7 \times 10^{-3} \text{ yr}^{-1}$ . If we assume the lifetime of HD 265435-like systems is about 55 Myr (stage 7 to stage 8 in Figure 3), the number of HD 265435-like systems in the Milky Way is likely to be 44 000–203500. According to the result of Liu et al. (2018b), the delay time of SNe Ia from HD 265435-like systems ranges from 110 Myr to the Hubble time for the case with  $\alpha_{CE}\lambda=1.0$ , which means that this channel could produce SNe Ia with short, intermediate, long delay times.

The mass-transfer processes, especially CE phases, are crucial for the formation of CO WD+He star systems. Because the CE ejection is still uncertain, we also check the influence of difference values of  $\alpha_{CE}$  on the distribution of the orbital periods. Figure 6 presents the orbital period distributions of CO WD+He star binaries for different values of  $\alpha_{CE}$ . From this figure, we can see that the orbital period  $P_{orb}$  is in the range of 0.01–10.0 days. For the cases with  $\alpha_{CE}=1$  and 2, the peaks are at around 0.05 days, while the peak is at 0.1 days for the case with  $\alpha_{CE}=3$ . The orbital period tends to be larger and more CO WD + He star systems would be produced when the value of  $\alpha_{CE}$  increases. This is because the CE ejection would release less orbital energy and happen more easily for a larger  $\alpha_{CE}$ .

In the present work, we employ the Monte Carlo BPS method to evolve a large number of primordial binaries to CO WD+He star systems and provide the distribution of CO WD +He star systems. We also reproduce the evolutionary history of HD 265435 and give a possible future evolution. It seems that HD 265435 originates from a primordial binary consisting of a  $5.18 M_{\odot}$  primary and a  $3.66 M_{\odot}$  secondary with an initial orbital period of 5200 days. Now and in the future, HD 265435 may be observed by some future space-based gravitational wave observatories, like LISA, TianQin and Taiji. The present

work indicates that HD 265435 is a strong progenitor candidate of SNe Ia and a potential target for space-based gravitational wave observatories.

## Acknowledgments

We acknowledge useful comments and suggestions from the anonymous referee. This study is supported by the National Key R&D Program of China (Nos. 2021YFA1600404 and 2021YFA1600403), the National Natural Science Foundation of China (Nos. 12225304 and 12273105), the Western Light Project of CAS (No. XBZG-ZDSYS-202117), the science research grants from the China Manned Space Project (Nos. CMS-CSST-2021-A12/B07), the Youth Innovation Promotion Association CAS (No. 2021058), and the Yunnan Fundamental Research Projects (Nos. 202001AS070029, 202001AU070054, 202101AT070027 and 202101AW070047).

## ORCID iDs

Bo Wang  <https://orcid.org/0000-0002-3231-1167>

## References

- Abbott, B. P., Abbott, R., Abbott, T. D., et al. 2016, *PhRvL*, **116**, 061102
- Ablimit, I. 2022, *MNRAS*, **509**, 6061
- Ablimit, I., & Maeda, K. 2019, *ApJ*, **871**, 31
- Ablimit, I., Xu, X.-j., & Li, X. D. 2014, *ApJ*, **780**, 80
- Ashok, N. M., & Banerjee, D. P. K. 2003, *A&A*, **409**, 1007
- Badenes, C., Hughes, J. P., Bravo, E., & Langer, N. 2007, *ApJ*, **662**, 472
- Cao, Y., Kulkarni, S. R., Howell, D. A., et al. 2015, *Natur*, **521**, 328
- Chen, W.-C. 2020, *ApJ*, **896**, 129
- Chen, W.-C. 2022, *A&A*, **662**, A79
- Chen, W.-C., & Li, X.-D. 2007, *ApJL*, **658**, L51
- Chen, W.-C., & Li, X.-D. 2009, *ApJ*, **702**, 686
- Danzmann, K. & LISA Study Team 1997, *CQGra*, **14**, 1399
- Dilday, B., Howell, D. A., Cenko, S. B., et al. 2012, *Sci*, **337**, 942
- Eggleton, P. P. 1973, *MNRAS*, **163**, 279
- Eggleton, P. P., & Kiseleva-Eggleton, L. 2002, *ApJ*, **575**, 461
- Fang, J., & Zhang, L. 2012, *MNRAS*, **424**, 2811
- Filippenko, A. V. 1997, *ARA&A*, **35**, 309
- Ganeshalingam, M., Li, W., & Filippenko, A. V. 2011, *MNRAS*, **416**, 2607
- Geier, S., Nesslinger, S., Heber, U., et al. 2007, *A&A*, **464**, 299
- Graur, O., Bianco, F. B., Huang, S., et al. 2017, *ApJ*, **837**, 120
- Greggio, L., & Renzini, A. 1983, *A&A*, **118**, 217
- Hachisu, I., Kato, M., & Nomoto, K. 1996, *ApJL*, **470**, L97
- Han, Z., & Podsiadlowski, P. 2004, *MNRAS*, **350**, 1301
- Han, Z., Podsiadlowski, P., & Eggleton, P. P. 1994, *MNRAS*, **270**, 121
- Han, Z., Podsiadlowski, P., & Eggleton, P. P. 1995, *MNRAS*, **272**, 800
- Hancock, P. J., Gaensler, B. M., & Murphy, T. 2011, *ApJL*, **735**, L35
- Hicken, M., Garnavich, P. M., Prieto, J. L., et al. 2007, *ApJL*, **669**, L17
- Hoefflich, P., Khokhlov, A., Wheeler, J. C., et al. 1996, *ApJL*, **472**, L81
- Horesh, A., Kulkarni, S. R., Fox, D. B., et al. 2012, *ApJ*, **746**, 21
- Howell, D. A., Sullivan, M., Nugent, P. E., et al. 2006, *Natur*, **443**, 308
- Hu, W.-R., & Wu, Y.-L. 2017, *Nat Sci. Rev.*, **4**, 685
- Hurley, J. R., Tout, C. A., & Pols, O. R. 2002, *MNRAS*, **329**, 897
- Iben, I. J., & Tutukov, A. V. 1984, *ApJS*, **54**, 335
- Israel, G. L., Stella, L., Angelini, L., et al. 1997, *ApJL*, **474**, L53
- Ivanova, N., Justham, S., Chen, X., et al. 2013, *A&ARv*, **21**, 59
- Kasen, D. 2010, *ApJ*, **708**, 1025
- Kato, M., & Hachisu, I. 2003, *ApJL*, **598**, L107
- Kerzendorf, W. E., Schmidt, B. P., Asplund, M., et al. 2009, *ApJ*, **701**, 1665
- Kraft, R. P., Mathews, J., & Greenstein, J. L. 1962, *ApJ*, **136**, 312

- Langer, N., Deutschmann, A., Wellstein, S., & Höflich, P. 2000, *A&A*, **362**, 1046
- Leonard, D. C. 2007, *ApJ*, **670**, 1275
- Li, X. D., & van den Heuvel, E. P. J. 1997, *A&A*, **322**, L9
- Liu, D. D., Wang, B., Podsiadlowski, P., & Han, Z. 2016, *MNRAS*, **461**, 3653
- Liu, D., & Wang, B. 2020, *MNRAS*, **494**, 3422
- Liu, D., Wang, B., Chen, W., Zuo, Z., & Han, Z. 2018a, *MNRAS*, **477**, 384
- Liu, D., Wang, B., & Han, Z. 2018b, *MNRAS*, **473**, 5352
- Liu, D., Wang, B., Ge, H., Chen, X., & Han, Z. 2019, *A&A*, **622**, A35
- Liu, J., Di Stefano, R., Wang, T., & Moe, M. 2012, *ApJ*, **749**, 141
- Liu, W. M., Chen, W. C., Wang, B., & Han, Z. W. 2010, *A&A*, **523**, A3
- Liu, Z.-W., Moriya, T. J., & Stancliffe, R. J. 2015, *MNRAS*, **454**, 1192
- Luo, J., Chen, L.-S., Duan, H.-Z., et al. 2016, *CQGra*, **33**, 035010
- Maoz, D., & Mannucci, F. 2012, *PASA*, **29**, 447
- Maoz, D., Mannucci, F., & Nelemans, G. 2014, *ARA&A*, **52**, 107
- Marion, G. H., Brown, P. J., Vinkó, J., et al. 2016, *ApJ*, **820**, 92
- Matteucci, F., & Greggio, L. 1986, *A&A*, **154**, 279
- Maxted, P. F. L., Marsh, T. R., & North, R. C. 2000, *MNRAS*, **317**, L41
- McCully, C., Jha, S. W., Foley, R. J., et al. 2014, *Natur*, **512**, 54
- Mennekens, N., Vanbeveren, D., De Greve, J. P., & De Donder, E. 2010, *A&A*, **515**, A89
- Mereghetti, S., Pintore, F., Esposito, P., et al. 2016, *MNRAS*, **458**, 3523
- Miller, G. E., & Scalzo, J. M. 1979, *ApJS*, **41**, 513
- Nelemans, G., Yungelson, L. R., Portegies Zwart, S. F., & Verbunt, F. 2001, *A&A*, **365**, 491
- Nomoto, K. 1982, *ApJ*, **253**, 798
- Nomoto, K., & Iben, I. J. 1985, *ApJ*, **297**, 531
- Nomoto, K., Thielemann, F. K., & Yokoi, K. 1984, *ApJ*, **286**, 644
- Nugent, P., Baron, E., Branch, D., Fisher, A., & Hauschildt, P. H. 1997, *ApJ*, **485**, 812
- Olling, R. P., Mushotzky, R., Shaya, E. J., et al. 2015, *Natur*, **521**, 332
- Pakmor, R., Hachinger, S., Röpke, F. K., & Hillebrandt, W. 2011, *A&A*, **528**, A117
- Patat, F., Chandra, P., Chevalier, R., et al. 2007, *Sci*, **317**, 924
- Pelisolì, I., Neunteufel, P., Geier, S., et al. 2021, *NatAs*, **5**, 1052
- Perlmutter, S., Aldering, G., Goldhaber, G., et al. 1999, *ApJ*, **517**, 565
- Podsiadlowski, P., Mazzali, P., Lesaffre, P., Han, Z., & Förster, F. 2008, *NewAR*, **52**, 381
- Pols, O. R., Schröder, K.-P., Hurley, J. R., Tout, C. A., & Eggleton, P. P. 1998, *MNRAS*, **298**, 525
- Pols, O. R., Tout, C. A., Eggleton, P. P., & Han, Z. 1995, *MNRAS*, **274**, 964
- Riess, A. G., Filippenko, A. V., Challis, P., et al. 1998, *AJ*, **116**, 1009
- Ruiter, A. J., Sim, S. A., Pakmor, R., et al. 2013, *MNRAS*, **429**, 1425
- Scalzo, R. A., Aldering, G., Antilogus, P., et al. 2010, *ApJ*, **713**, 1073
- Schaefer, B. E., & Pagnotta, A. 2012, *Natur*, **481**, 164
- Silverman, J. M., Ganeshalingam, M., Li, W., et al. 2011, *MNRAS*, **410**, 585
- Silverman, J. M., Nugent, P. E., Gal-Yam, A., et al. 2013, *ApJS*, **207**, 3
- Sternberg, A., Gal-Yam, A., Simon, J. D., et al. 2011, *Sci*, **333**, 856
- Tauris, T. M. 2018, *PhRvL*, **121**, 131105
- Tutukov, A. V., & Yungelson, L. R. 1981, *Nauchnye Informatsii*, **49**, 3
- Voss, R., & Nelemans, G. 2008, *Natur*, **451**, 802
- Wang, B., Chen, X., Meng, X., & Han, Z. 2009a, *ApJ*, **701**, 1540
- Wang, B., Meng, X., Chen, X., & Han, Z. 2009b, *MNRAS*, **395**, 847
- Wang, B., & Han, Z. 2012, *NewAR*, **56**, 122
- Wang, B., & Han, Z.-W. 2010a, *RAA*, **10**, 681
- Wang, B., & Han, Z.-W. 2010b, *RAA*, **10**, 235
- Wang, B., Podsiadlowski, P., & Han, Z. 2017, *MNRAS*, **472**, 1593
- Wang, X., Wang, L., Filippenko, A. V., Zhang, T., & Zhao, X. 2013, *Sci*, **340**, 170
- Wang, X., Filippenko, A. V., Ganeshalingam, M., et al. 2009c, *ApJL*, **699**, L139
- Wang, X., Wang, L., Filippenko, A. V., et al. 2012, *ApJ*, **749**, 126
- Webbink, R. F. 1984, *ApJ*, **277**, 355
- Whelan, J., & Iben, I. J. 1973, *ApJ*, **186**, 1007
- Williams, B. J., Blair, W. P., Blondin, J. M., et al. 2011, *ApJ*, **741**, 96
- Woudt, P. A., & Steeghs, D. 2005, in ASP Conf. Ser., 330, *The Astrophysics of Cataclysmic Variables and Related Objects*, ed. J. M. Hameury & J. P. Lasota (San Francisco, CA: ASP), 451
- Xu, X.-j., Wang, Q. D., & Li, X. 2022, *MNRAS*, **516**, 1263
- Yoon, S. C., & Langer, N. 2003, *A&A*, **412**, L53
- Yoon, S. C., Podsiadlowski, P., & Rosswog, S. 2007, *MNRAS*, **380**, 933